

# Investigation of Domain Size in Polymer Membranes Using Double-Quantum-Filtered Spin Diffusion Magic Angle Spinning NMR

B. R. Cherry,<sup>†</sup> C. H. Fujimoto, C. J. Cornelius, and T. M. Alam\*

Sandia National Laboratories, MS 0886, Albuquerque, New Mexico 87185-0886

Received October 12, 2004; Revised Manuscript Received November 23, 2004

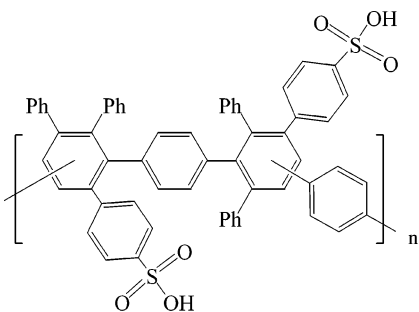
**ABSTRACT:** Solid-state  $^1\text{H}$  magic angle spinning (MAS) NMR was used to investigate sulfonated Diels–Alder poly(phenylene) polymer membranes. Under high spinning speed  $^1\text{H}$  MAS conditions, the proton environments of the sulfonic acid and phenylene polymer backbone are resolved. A double-quantum (DQ) filter using the rotor-synchronized back-to-back (BABA) NMR multiple-pulse sequence allowed the selective suppression of the sulfonic proton environment in the  $^1\text{H}$  MAS NMR spectra. This DQ filter in conjunction with a spin diffusion NMR experiment was then used to measure the domain size of the sulfonic acid component within the membrane. In addition, the temperature dependence of the sulfonic acid spin–spin relaxation time ( $T_2$ ) was determined, providing an estimate of the activation energy for the proton dynamics of the dehydrated membrane.

## 1. Introduction

Understanding the structure and morphology of proton exchange membranes (PEMs) is important in developing a complete understanding of the processes involved during charge conduction. Varieties of techniques have been employed to elucidate the structure of PEMs, including scattering (SAXS and SANS),<sup>1–4</sup> spectroscopic (NMR, IR, and Raman)<sup>5–8</sup> and microscopic (AFM, SEM, and TEM).<sup>8,9</sup> From a material science perspective, PEMs are generally characterized for thermal stability (DSC and TGA), solvent uptake, and ion exchange capacity (IEC), a measure of proton conductivity.<sup>8,10</sup>

Perfluorinated PEMs (e.g., Nafion) are limited by low performance at temperatures above 80 °C, fuel permeation, high production costs, and environmental processing issues. These limitations have initiated the search for cheaper and more robust alternatives. Polyphenylenes represent a class of materials with high thermal and chemical stability and are easily functionalized.

Recently, the potential of sulfonated Diels–Alder polyphenylene-based PEMs was demonstrated.<sup>11</sup> This study revealed that these materials possessed proton conductivities up to 60 mS/cm (Nafion, 88 mS/cm) and were thermally stable up to 200 °C. The Diels–Alder membrane material consists of a polyphenylene backbone with sulfonic acid functionalized phenyl side chains. This material is expected to have the following monomer repeat unit:



For the polymer studied in this paper, 65% of the repeat units contained the  $-\text{SO}_3\text{H}$  functionalities. The impact of sulfonic acid heterogeneities within the membrane is expected to impact the observed proton conductivity, but has yet to be fully explored.

High-speed ( $> 30$  kHz)  $^1\text{H}$  magic angle spinning (MAS) NMR techniques have recently proven to be an important tool for the structure determination of polymer materials.<sup>12</sup> The high spinning speeds provide significant averaging of the strong  $^1\text{H}$ – $^1\text{H}$  dipolar coupling, allowing for enhanced chemical shift resolution on rigid samples that otherwise would suffer from broad, non-informative  $^1\text{H}$  NMR spectra. Furthermore, advanced multipulse dipolar recoupling experiments have been developed to selectively reintroduce the  $^1\text{H}$ – $^1\text{H}$  dipolar coupling, allowing through space correlation between protons and other structural information to be obtained.<sup>13–15</sup>

Another advance that has greatly improved the usefulness of NMR to the pursuit of polymer structure (in particular) is the utilization of spin diffusion to probe length scales of heterogeneous domains, from tens of angstroms to hundreds of nanometers.<sup>16–18</sup> Spin diffusion techniques have been used to probe a multitude of advanced materials.<sup>18–25</sup> A strength of spin diffusion is that it does not rely on how magnetization of a spin domain is generated as long as one type of domain can be selected over another. The process then allows magnetization to transfer (analogous to a diffuse manner) from the “source” region to the “drain” region, providing accurate information on the size of each domain to be obtained.<sup>18,26,27</sup>

A variety of techniques have been developed to select magnetization from one domain versus another within the polymer. These include differences in line width, dipolar filters (based on differences in spin relaxation parameters  $T_2$  and  $T_{1\rho}$ ), and chemical shift.<sup>23,28,29</sup> Double-quantum (DQ) filters have also been utilized,<sup>26,30–35</sup> where DQ refers to the coherence order created as a result of dipolar interactions between two (or more) coupled nuclei (such as  $^1\text{H}$  or  $^{13}\text{C}$ ) within the material. The DQ filter is unique in that it retains magnetization from the component with the stronger dipolar couplings (rigid phase) and suppresses the signal of the components with weaker dipolar couplings (mobile phase), in

\* To whom correspondence should be addressed. Fax: (505) 844-9624. E-mail: tmalam@sandia.gov.

<sup>†</sup> Current address: Bruker Biospin, Billerica, MA.

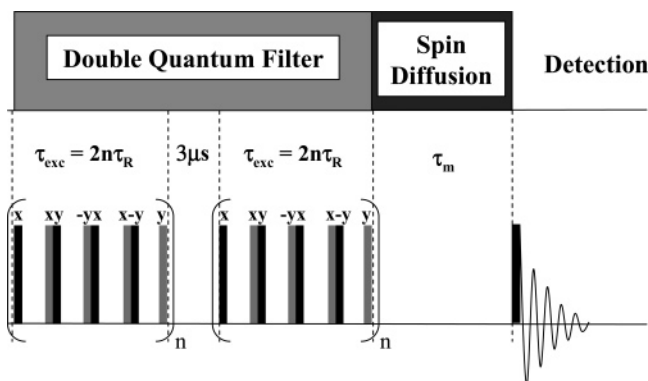


**Figure 1.** Double-quantum-filtered  $^1\text{H}$  MAS NMR spin diffusion experiment utilizing the rotor-synchronized BABA excitation/conversion sequence. The excitation period  $\tau_{\text{exc}}$  is an even multiple of the rotor period  $\tau_r$ . Variation in the mixing time  $\tau_m$  allows monitoring of  $^1\text{H}$ – $^1\text{H}$  spin diffusion within the material.

contrast to the dipolar filter, which suppresses the signal from the components with strong dipolar couplings (rigid phase).<sup>34,35</sup> In the DQ filter, the suppressed component has a small (or zero) dipolar coupling due to lack of coupling partners spatially near within the material, or has a weak dipolar coupling as a result of rapid motional averaging of internal dipolar couplings. Selection may also occur from interference effects between internal motions on the time scale of the DQ excitation/reconversion pulse sequence employed.

The DQ filter was first introduced into NMR spin diffusion experiments by Ba and Ripmesster on static samples of adamantane/benzene- $d_6$  and high-density polyoxymethylene (HD POM),<sup>30</sup> utilizing the MQ excitation scheme with time reversal of Yen and Pines.<sup>31</sup> Buda et al.<sup>32</sup> validated the use of a four-pulse DQ filter under static conditions to select magnetization for spin diffusion measurements, by comparing the results from the DQ-filtered method to those of traditional dipolar-selected spin diffusion methods of well-characterized diblock copolymers of polystyrene–poly(ethylene oxide) (PS–PEO) and poly(hydroxyethyl methacrylate)–poly(ethylene oxide) (PHEMA–PEO). They also demonstrated that the characteristic spin diffusion value  $(\tau_m^*)^{1/2}$ , used to extract distance information, does not depend on the efficiency of the DQ filter. More recently, Buda and co-workers utilized  $^1\text{H}$  DQ-filtered NMR spin diffusion experiments to probe the morphology of Nylon-6 fibers.<sup>26,33</sup>

In this paper, we describe the use of the rotor-synchronized, back-to-back (BABA) multipulse train for the excitation/reconversion component of a DQ-filtered  $^1\text{H}$  MAS NMR spin diffusion experiment as shown in Figure 1. By utilizing the BABA sequence, the increased spectral resolution obtained from high-speed MAS is retained, while maintaining high double-quantum/single-quantum conversion efficiency. The spin diffusion between the different selected  $^1\text{H}$  domains can now be monitored by obtaining NMR spectra for different mixing times,  $\tau_m$  (Figure 1). As a demonstration this DQ-filtered  $^1\text{H}$  MAS NMR spin diffusion experiment was used to measure the sulfonic acid moiety domain size in a sulfonated Diels–Alder polyphenylene polymer membrane.

## 2. Experimental Section

The sulfonated Diels–Alder polyphenylene membrane material was synthesized from the polymerization of 1,4-bis(2,4,5-

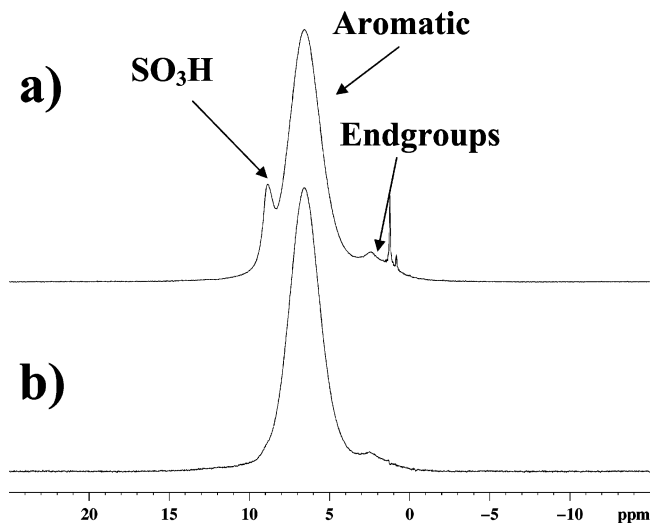


**Figure 2.** (a) High-speed (30 kHz)  $^1\text{H}$  MAS NMR spectrum and (b) DQ-filtered  $^1\text{H}$  MAS NMR spectrum of the Diels–Alder membrane material obtained at 328 K. Small organic impurities are denoted with an asterisk.

triphenylcyclopentadienone)benzene and 1,4-diethynylbenzene followed by postsulfonation using chlorosulfonic acid as described elsewhere.<sup>11</sup> The resulting material was cast on glass plates and then washed with deionized water to remove any excess acid.<sup>11</sup> These membrane samples were then removed from the glass substrate, dehydrated, packed in an MAS NMR rotor, and stored over  $\text{P}_2\text{O}_5$  in an inert glovebox prior to the NMR investigation.

The  $^1\text{H}$  MAS NMR experiments were carried out on a Bruker Avance spectrometer at a Larmor frequency of 600.1 MHz. All experiments were performed on a 2.5 mm MAS probe, with 30 kHz spinning speed, and a 13 s recycle delay. The DQ filter spin diffusion pulse sequence (shown in Figure 1) utilizes the BABA excitation/reconversion sequence introduced by Fiege and co-workers.<sup>36</sup> The excitation/reconversion was applied for 2 rotor periods ( $2\tau = 66.67 \mu\text{s}$ ), each with a fixed  $3 \mu\text{s}$  delay between the excitation and reconversion of the DQ coherence, utilizing a  $3 \mu\text{s}$   $\pi/2$  pulse, 128 scans, 2 dummy scans, and 39 spin diffusion mixing periods ( $\tau_m$ ) ranging from  $50 \mu\text{s}$  to 300 ms. The 2D nuclear Overhauser enhancement spectroscopy (NOESY)<sup>37,38</sup> MAS NMR experiment utilized a 5 ms mixing period for spin diffusion. The effective spin–spin relaxation times ( $T_2^*$ ) were measured utilizing a rotor-synchronized Hahn-echo, with echo delays of 1–6 rotor periods at different sample temperatures. All reported temperatures were corrected for the additional frictional heating caused by high-speed spinning, on the basis of temperature calibrations using  $\text{PbNO}_3$ . For example, at a room temperature of 294 K, the actual sample temperature was determined to be 328 K at a 30 kHz spinning speed. The  $^1\text{H}$  chemical shifts were referenced to a  $\text{H}_2\text{O}$  secondary standard ( $\delta = +4.8$  ppm with respect to the peak for tetramethylsilane,  $\delta = 0$  ppm) at 298 K.

## 3. Results and Discussion

**3.1. Characterization and Assignment of the  $^1\text{H}$  MAS NMR Spectrum.** The high-speed (30 kHz)  $^1\text{H}$  MAS NMR spectrum of the sulfonated Diels–Alder polyphenylene membrane at 328 K is shown in Figure 2a. Three resonances associated with the polymer material are resolved, with the resonances at  $\delta = +6.5$  and  $+2.5$  ppm being assigned to the aromatic and end groups of the polymer backbone, respectively, while the resonance at  $\delta = +8.9$  ppm is assigned to the sulfonic acid proton. It has been well established that the observed  $^1\text{H}$  NMR chemical shift is a measure of hydrogen bond strength,<sup>39,40</sup> with the chemical shifts of

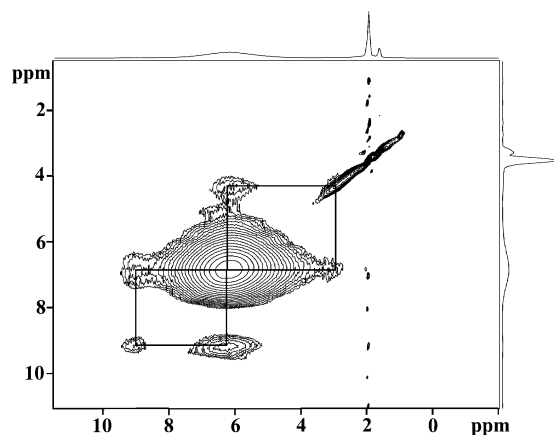


**Figure 3.** 2D  $^1\text{H}$  NOESY MAS NMR exchange spectra of the membrane using a 5 ms mixing period at 328 K. The exchange of magnetization due to spatial connectivity between the different  $^1\text{H}$  resonances within the polymer membrane is observed.

acid protons typically between +10 and +20 ppm. The observed +8.9 ppm  $^1\text{H}$  chemical shift of the sulfonic acid group suggests relatively weak hydrogen-bonding interactions. The presence of low concentrations of water within the polyphenylene membrane may also reduce the observed chemical shift due to exchange averaging between the water and acid resonances. On the other hand, it is known that for hydrated multilayer films containing poly(sodium styrenesulfonate), the bulk water resonance is readily observable under MAS conditions with a  $^1\text{H}$  chemical shift ranging from +4.3 to 3.4 ppm depending on the relative water concentration per sulfonate group.<sup>6</sup> Bulk water is not observed in the  $^1\text{H}$  MAS NMR of the sulfonated Diels–Alder polyphe-nylene membranes reported here. While it is extremely difficult to fully remove the water in these sulfonated membranes, weight loss experiments under  $\text{P}_2\text{O}_5$  desiccation and vacuum allow the estimation of the water concentration to be less than 5% of the acid proton concentration. The sharp resonances near +1 ppm are organic impurities, but represent a very minor concentration.

The DQ-filtered MAS NMR spectrum for the polymer using a  $2\tau = 66.67 \mu\text{s}$  excitation/reconversion period is also shown in Figure 2b. The DQ filter removes resonances with weak dipolar coupling, resulting from either long spatial proximity ( $>5 \text{ \AA}$ ) or averaging due to rapid motional averaging. To confirm that the three  $^1\text{H}$  resonances are spatially close and part of the same polymer chain, a 2D NOESY<sup>37,38</sup> MAS NMR exchange experiment was also preformed and is shown in Figure 3. Correlation peaks were observed between the aromatic ( $\delta = +6.5 \text{ ppm}$ ) and end group ( $\delta = +2.5 \text{ ppm}$ ) resonances and between the aromatic and sulfonic acid ( $\delta = +8.9 \text{ ppm}$ ) resonances, indicating close spatial connectivity between these  $^1\text{H}$  environments within the membrane. Attempts to select the sulfonic acid protons on the basis of differences in spin–spin relaxation times ( $T_2$ ) using a  $T_2$ -dipolar filter were not successful due to the similarity in  $T_2$  values for the different  $^1\text{H}$  domains (see below). Similarly,  $^1\text{H}$ – $^1\text{H}$  spin diffusion experiments using  $^1\text{H}$ – $^{13}\text{C}$  correlation experiments as described for other polymer systems<sup>27</sup> are not readily applicable to the Diels–Alder membrane since the sulfonic acid portion of the polymer does not contain carbon nuclei. These results demonstrate one of the benefits of the DQ filter in its ability to separate

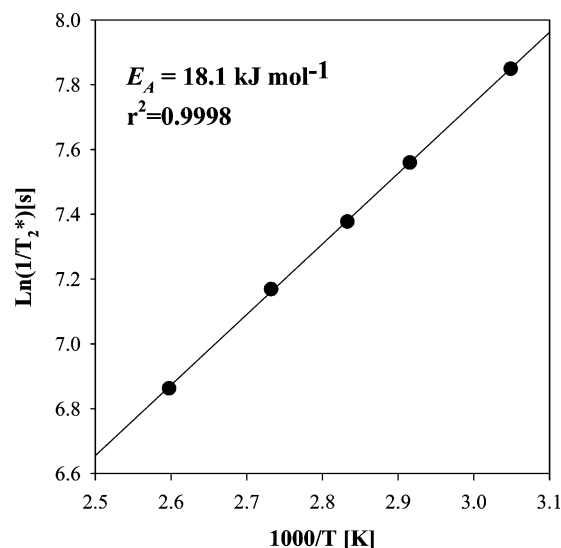


**Figure 4.** Arrhenius plot of the temperature dependence of the NMR spin–spin relaxation time  $T_2^*$  for the sulfonic acid resonance ( $\delta = +8.9 \text{ ppm}$ ) in the Diels–Alder membrane, giving an activation energy of  $E_A \approx 18 \text{ kJ mol}^{-1}$ .

different  $^1\text{H}$  environments without relying on differences in domain mobility.

When local motions are fast on the NMR time scale, the  $T_2$  relaxation time is related to the correlation time for those motions.<sup>15</sup> Under high-speed MAS NMR conditions, an effective spin–spin relaxation time ( $T_2^*$ ) was measured for each  $^1\text{H}$  resonance within the membrane as a function of sample temperature. For the aromatic backbone protons ( $\delta = +6.5 \text{ ppm}$ )  $T_2^* \approx 350 \mu\text{s}$  and was constant over the temperature range explored, while the  $T_2^*$  of the sulfonic acid proton ( $\delta = +8.9 \text{ ppm}$ ) showed a pronounced temperature dependence, varying from  $390 \mu\text{s}$  at 328 K to 1.05 ms at 385 K. Again note that the similarity of  $T_2^*$  at 328 K between the aromatic and sulfonic acid protons precludes the use of a dipolar filter for selection of the different  $^1\text{H}$  domains.

In the motional narrowing limit,<sup>41</sup> the temperature dependence of the sulfonic acid proton  $T_2^*$  is a probe of proton mobility on the microscopic scale and is argued to arise from proton hopping following an Arrhenius relation:<sup>42</sup>

$$\frac{1}{T_2^*} \approx \tau_c = \tau_\infty \exp\left(\frac{E_A}{RT}\right) \quad (1)$$

Figure 4 is a plot of the  $\ln(1/T_2^*)$  as a function of reduced temperature, allowing a proton hopping activation energy  $E_A \approx 18 \text{ kJ mol}^{-1}$  to be determined. Previous studies on imidazole-based PEMs were the first to show that the temperature dependence of  $T_2$  and that of the conductivity (macroscopic scale) can be utilized to relate the microscopic and macroscopic proton transport processes.<sup>15</sup> A direct comparison of conductivity measurements and NMR relaxation is not straightforward.<sup>15</sup> However, large differences in the macroscopic and microscopic activation energy will indicate that processes in addition to the local sulfonic acid motions (Grothuss hopping) contribute to the conductivity (e.g., vehicle transport).<sup>5,43</sup> In the imidazole-based system, a factor of 3 increase of the macroscopic activation energy (from conductivity,  $128 \text{ kJ mol}^{-1}$ ) over the microscopic activation energy (from NMR,  $48 \text{ kJ mol}^{-1}$ ) was the result of the system being comprised of two domains,



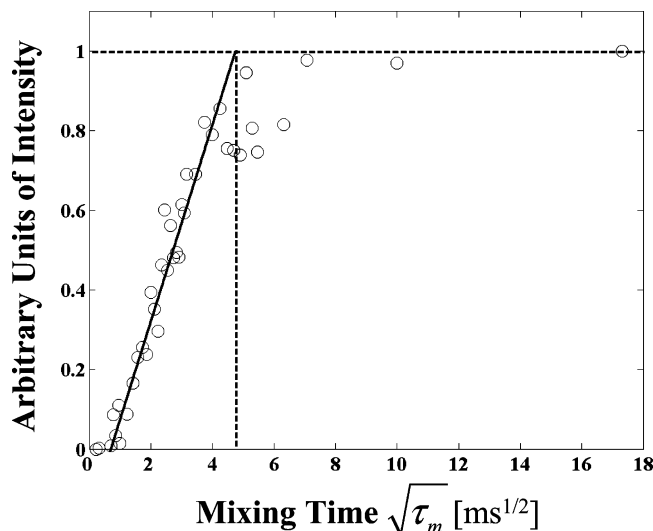


**Figure 5.** NMR spectral intensity of the sulfonic acid resonance ( $\delta = +8.9$  ppm) as a function of the square root of the spin diffusion mixing time. The solid line is the linear regression best fit to the initial buildup of magnetization, giving an estimate of  $(\tau_m^*)^{1/2}$ .

disordered (mobile) and crystalline (rigid). Proton conduction through the crystalline domains was inhibited due to strong hydrogen bonding; therefore, the macroscopic activation energy for charge transport is greater than the local proton mobility (NMR determined) suggests.<sup>15</sup> In the dehydrated Diels–Alder material of the present study, the activation energy determined by NMR relaxation experiments ( $\sim 18$  kJ mol<sup>-1</sup>) provides insights into the conduction arising from Grotthuss hopping of protons between sulfonic acid moieties. The activation energy will also be a function of water concentration, but was not investigated here. Conductivity measurements of these sulfonated Diels–Alder membranes with temperature are not presently available. Bulk conductivity studies on membranes as a function of temperature and hydration will provide information on the magnitude of vehicle-mediated transport occurring in the membrane, and is an area of future work.

### 3.2. DQ-Filtered <sup>1</sup>H MAS NMR Spin Diffusion.

The morphology of the sulfonic acid group portion of the polymer has been proposed as one factor that may influence the observed <sup>1</sup>H conductivity.<sup>11</sup> To explore this issue, the BABA DQ-filtered <sup>1</sup>H MAS NMR spin diffusion pulse sequence depicted in Figure 1 was used to investigate the sulfonic acid domain size of the dehydrated sulfonated Diels–Alder polyphenylene membrane. The DQ filter selected <sup>1</sup>H magnetization from the polymer backbone protons ( $\delta = +2.5$  and  $+6.5$  ppm), while significantly suppressing the <sup>1</sup>H signal from the sulfonic acid group (Figure 2b). During the subsequent mixing period ( $\tau_m$ ) magnetization transfer via <sup>1</sup>H–<sup>1</sup>H spin diffusion to the sulfonic acid protons ( $\delta = +8.9$  ppm) occurs, resulting in an increase of the acid signal intensity. Figure 5 shows the DQ-filtered <sup>1</sup>H spin diffusion buildup curve for the sulfonic acid proton resonance as a function of mixing time. From the initial buildup rate of the spin diffusion data an estimation of the hydrophilic sulfonic acid domain size can be made (see below). It should be noted that even for the longest mixing time (300 ms) the sharp resonances near 1 ppm, assigned to sample impurities, never returned to the DQ-filtered spin diffusion spectra, indicating that these

resonances are not directly associated with the Diels–Alder membrane material.

Methods for determining domain size from spin diffusion data range from an approximation based on the initial rate of magnetization buildup, to analytic solutions of the diffusion equation.<sup>18,23,26,44,45</sup> All methods are predicated from a reliable value for the proton spin diffusion coefficient, which is proportional to the through-space dipolar coupling of the protons within the sample. Spectral line widths have been used as indirect measures of the spin diffusion coefficient. However, spectral overlap of proton species with different chemical shifts will result in an overestimation of the residual dipolar coupling. Determination of spin diffusion coefficients based on the effective spin–spin relaxation rate  $[(T_2^*)^{-1}]$  eliminates this overestimation, and is given by<sup>46</sup>

$$D[(T_2^*)^{-1}] = (4.5 \times 10^{-5})[T_2^*(s)]^{-1} + 0.26 \quad (2)$$

On the basis of  $(T_2^*)^{-1}$  of the aromatic (350  $\mu$ s) and sulfonic acid (390  $\mu$ s) protons, the spin diffusion coefficient  $D[(T_2^*)^{-1}]$  at 328 K was determined to be 0.39 and 0.38 nm<sup>2</sup> ms<sup>-1</sup>, respectively. Since the  $T_2^*$  values are dependent on the MAS spinning speed and sample temperature, the effective spin diffusion coefficient is also spinning speed and temperature dependent. For the present study all spin diffusion experiments were performed at a sample temperature of 328 K.

For a two-phase system in which one phase is dispersed within a matrix, the domain size ( $d$ ) of the dispersed or minor phase is given by<sup>18,23,44</sup>

$$d = \left( \frac{\rho_{\text{HA}}\phi_A + \rho_{\text{HB}}\phi_B}{\phi_A\phi_B} \right) \left( \frac{4\epsilon\phi_A}{\pi^{1/2}} \right) \left( \frac{(D_A D_B)^{1/2}}{\rho_{\text{HA}}D_A^{1/2} + \rho_{\text{HB}}D_B^{1/2}} \right) (\tau_m^*)^{1/2} \quad (3)$$

where  $\rho_H$  is the proton density,  $\phi$  is the volume fraction, and  $D$  is the spin diffusion coefficient for the two phases (A and B), where A is the dispersed phase. The dimensionality of the system is defined by  $\epsilon$ , and  $(\tau_m^*)^{1/2}$  is the mixing time that corresponds to intersection of the initial magnetization buildup with the equilibrium magnetization intensity.

For the sulfonated Diels–Alder membrane material the volume fractions are given by  $\phi_A = 0.041$  and  $\phi_B = 0.959$ , and the proton densities by  $\rho_{\text{HA}} = 0.029$  g/cm<sup>3</sup> and  $\rho_{\text{HB}} = 0.057$  g/cm<sup>3</sup>, for the sulfonic acid and aromatic domain, respectively. Extrapolation of the initial buildup of magnetization to the intersection with the equilibrium magnetization intensity results in a  $(\tau_m^*)^{1/2}$  value of 4.67 ms<sup>1/2</sup> (see Figure 5). This rapid spin diffusion buildup is consistent with intramolecular magnetization transfer one would expect for <sup>1</sup>H–<sup>1</sup>H spin diffusion within the same polymer unit.<sup>27</sup> In addition the lack of a delay in the spin diffusion curve suggests that there is a sharp interface between the two different proton domains, and that an interfacial region is not present. Using this initial rate approximation (eq 3), the hydrophilic sulfonic acid proton conduction domain size was determined to be  $\sim 4.4$ , 8.8, or 13.2 nm, depending on the dimensionality of the system ( $\epsilon = 1, 2$ , or 3).

The initial rate approximation suffers from the fact that it is unable to distinguish domain size effects from dimensionality effects.<sup>18,44</sup> Information about the domain dimensionality can be extracted from the full

diffusion curve through subtle differences in the recovery profile,<sup>18,44</sup> even though distributions in domain size or departure from periodic repeat structures makes these identifications very difficult.<sup>44</sup> The spin diffusion data present in Figure 5 are unable to provide details about the dimensionality of the domains within the Diels–Alder membrane. Therefore, additional information about the dimensionality of the hydrophilic domain present in the Diels–Alder membrane material (by either microscopy or small angle diffraction) is needed to accurately determine the overall domain size. Recent AFM studies of sulfonated poly(arylene ether sulfone) have shown that hydrophilic channel-like (2D) domains present are on the order of 10–25 nm in diameter.<sup>9</sup> This domain size is on the same order as the ~9 nm ( $\epsilon = 2$ ) measured by NMR for the Diels–Alder polyphenylene membrane in the present study. The reduced domain size observed in the dehydrated Diels–Alder membrane versus the fully hydrated poly(arylene ether sulfone) membranes studied by McGrath et al.<sup>9</sup> may be due to the different hydration levels. The variation of the measured domain size as a function of hydration level will be carefully explored in future work. The smaller relative size of the hydrophilic domain size in the Diels–Alder versus the poly(arylene ether sulfone) membranes may also result from the increased rigidity (reduced rotational freedom) of the polyphenylene backbone. Regardless of the actual dimensionality, the DQ-filtered <sup>1</sup>H MAS NMR experiments provide a size metric that can be used to compare properties of membranes produced under different synthetic and processing conditions, with observed changes in proton conductivity.

#### 4. Conclusion

High-speed <sup>1</sup>H MAS NMR provided good spectral resolution for a novel sulfonated Diels–Alder polyphenylene fuel cell membrane material. DQ-filtered <sup>1</sup>H MAS NMR allowed the identification and selection of the –SO<sub>3</sub>H protons. The temperature dependence of the spin–spin relaxation time  $T_2^*$  for the –SO<sub>3</sub>H protons predicts a proton hopping activation energy of ~18 kJ mol<sup>-1</sup>, and is consistent with this proton species being involved in conduction. A novel DQ-filtered <sup>1</sup>H MAS NMR spin diffusion experiment was used to determine the domain size of the sulfonic acid portion within the membrane. These DQ-filtered experiments allowed the utilization of high-speed MAS conditions for resolution of distinct chemical shifts, while providing a selection of magnetization based on the strength of dipolar coupling. Analogous experiments using a dipolar  $T_2$  filter were unsuccessful due to the similarity of the <sup>1</sup>H  $T_2^*$  in the different domains. Using these spin diffusion experiments, the domain size of the hydrophilic sulfonic acid region was found to be between 4 and 13 nm in size depending on the dimensionality. The correlation of domain size and observed conductivity in different membrane materials using this <sup>1</sup>H MAS NMR technique is an area of future research.

**Acknowledgment.** Sandia is a multiprogram laboratory operated by Sandia Corp., a Lockheed Martin Co., for the United States Department of Energy's National Nuclear Security Administration under Contract DE-AC04-94AL85000. This work is supported

under the Sandia Research Foundation and LDRD programs.

#### References and Notes

- (1) Haubold, H.-G.; Vad, T.; Jungbluth, H.; Hiller, P. *Electrochim. Acta* **2001**, *46*, 1559–1563.
- (2) Rollet, A.-L.; Diat, O.; Gebel, G. *J. Phys. Chem. B* **2002**, *106*, 3033–3036.
- (3) Paddison, S. J.; Paul, R. *Phys. Chem. Chem. Phys.* **2002**, *4*, 1158–1163.
- (4) Young, S. K.; Trevino, S. F.; Beck Tan, N. C. *J. Polym. Sci., Part B: Polym. Phys.* **2002**, *40*, 387–400.
- (5) Zawodzinski, T. A., Jr.; Neeman, M.; Sillerud, L. O.; Gottesfeld, S. *J. Phys. Chem.* **1991**, *95*, 6040–6044.
- (6) McCormick, M.; Smith, R. N.; Graf, R.; Barrett, C. J.; Reven, L.; Spiess, H. W. *Macromolecules* **2003**, *36*, 3616–3625.
- (7) Gruger, A.; Regis, A.; Schmatko, T.; Colomban, P. *Vib. Spectrosc.* **2001**, *26*, 215–225.
- (8) Smitha, B.; Sridhar, S.; Khan, A. A. *J. Membr. Sci.* **2003**, *225*, 63–76.
- (9) Wang, F.; Hickner, M.; Kim, Y. S.; Zawodzinski, T. A.; McGrath, J. E. *J. Membr. Sci.* **2002**, *197*, 231–242.
- (10) Zawodzinski, T. A., Jr.; Springer, T. E.; Uribe, F.; Gottesfeld, S. *Solid State Ionics* **1993**, *60*, 199–211.
- (11) Fujimoto, C. H.; Hickner, M. A.; Cornelius, C. J.; Loy, D. A. *Macromolecules*, in press.
- (12) Samoson, A.; Tuhern, T.; Gan, Z. *Solid State Nucl. Magn. Reson.* **2001**, *20*, 130–136.
- (13) Schnell, I.; Spiess, H. W. *J. Magn. Reson.* **2001**, *151*, 153–227.
- (14) Alam, T. M.; Fan, H. *Macromol. Chem. Phys.* **2003**, *204*, 2023–2030.
- (15) Goward, G. R.; Schuster, M. F. H.; Sebastiani, D.; Schnell, I.; Spiess, H. W. *J. Phys. Chem. B* **2002**, *106*, 9322–9334.
- (16) Goldman, M.; Shen, L. *Phys. Rev.* **1966**, *144*, 321–331.
- (17) Assink, R. A. *Macromolecules* **1978**, *11*, 1233–1237.
- (18) Clauss, J.; Schmidt-Rohr, K.; Spiess, H. W. *Acta Polym.* **1993**, *44*, 1–17.
- (19) Brus, J.; Dybal, J. *Polymer* **2000**, *41*, 5269–5282.
- (20) De Paul, S. M.; Zwanziger, J. W.; Ulrich, R.; Wiesner, U.; Spiess, H. W. *J. Am. Chem. Soc.* **1999**, *121*, 5727–5736.
- (21) Hu, W.-G.; Schmidt-Rohr, K. *Polymer* **2000**, *41*, 2979–2987.
- (22) Ulrich, R.; Zwanziger, J. W.; De Paul, S. M.; Reiche, A.; Leuninger, H.; Spiess, H. W.; Wiesner, U. *Adv. Mater.* **2002**, *14*, 1134–1137.
- (23) Schmidt-Rohr, K.; Spiess, H. W. *Multidimensional Solid-State NMR of Polymers*; Academic Press Limited: London; San Diego, CA, 1994.
- (24) Huster, D.; Yao, X.; Hong, M. *J. Am. Chem. Soc.* **2002**, *124*, 847–883.
- (25) Kretschmer, A.; Drake, R.; Neidhoefer, M.; Wilhelm, M. *Solid State Nucl. Magn. Reson.* **2002**, *22*, 204–217.
- (26) Buda, A.; Demco, D. E.; Bertmer, M.; Blümich, B.; Litvinov, V. M.; Penning, J. P. *J. Phys. Chem. B* **2003**, *107*, 5357–5370.
- (27) Jia, X.; Wolak, J.; Wang, X.; White, J. *Macromolecules* **2003**, *36*, 712–718.
- (28) Schmidt-Rohr, K.; Blümich, B.; Spiess, H. W. *Magn. Reson. Chem.* **1990**, *28*, 3.
- (29) Caravattii, P.; Neuenschwander, P.; Ernst, R. R. *Macromolecules* **1985**, *18*, 119.
- (30) Ba, Y.; Ripmeester, J. A. *J. Chem. Phys.* **1998**, *108*, 8589–8594.
- (31) Yen, Y.; Pines, A. *J. Chem. Phys.* **1983**, *78*, 3579–3582.
- (32) Buda, A.; Demco, D. E.; Bertmer, M.; Blümich, B.; Reining, B.; Keul, H.; Höcker, H. *Solid State Nucl. Magn. Reson.* **2003**, *24*, 39–67.
- (33) Buda, A.; Demco, D. E.; Blümich, B.; Litvinov, V. M.; Penning, J. P. *ChemPhysChem* **2004**, *5*, 876–883.
- (34) Graf, R.; Demco, D. E.; Gottwald, J.; Hafner, S.; Spiess, H. W. *J. Chem. Phys.* **1997**, *106*, 885–895.
- (35) Schnell, I. *Prog. Nucl. Magn. Reson.* **2004**, *45*, 145–207.
- (36) Fieke, M.; Demco, D. E.; Graf, R.; Gottwald, J.; Hafner, S.; Spiess, H. W. *J. Magn. Reson., A* **1996**, *122*, 214–221.
- (37) Macura, S.; Huang, Y.; Suter, D.; Ernst, R. R. *J. Magn. Reson.* **1981**, *43*, 259.

- (38) Jeener, J.; Meier, B. H.; Bachmann, P.; Ernst, R. R. *J. Chem. Phys.* **1979**, *71*, 4546–4553.
- (39) Jeffrey, G. A.; Yeon, Y. *Acta Crystallogr.* **1986**, *B42*, 410–413.
- (40) Harris, R. K.; Jackson, P.; Merwin, L. H.; Say, B. J.; Hägele, G. *J. Chem. Soc., Faraday Trans. 1* **1988**, *84*, 3649–3672.
- (41) Bloembergen, N.; Purcell, E. M.; Pound, R. V. *Phys. Rev.* **1948**, *73*, 679–712.
- (42) Slichter, C. P. *Principles of Magnetic Resonance*, 3rd ed.; Springer-Verlag: Berlin, 1990.
- (43) Kreuer, K. D.; Fuchs, A.; Ise, M.; Spaeth, M.; Maier, J. *Electrochim. Acta* **1998**, *43*, 1281–1288.
- (44) VanderHart, D. L.; McFadden, G. B. *Solid State Nucl. Magn. Reson.* **1996**, *7*, 45–66.
- (45) Wang, J. *J. Chem. Phys.* **1996**, *104*, 4850–4858.
- (46) Mellinger, F.; Wilhelm, M.; Spiess, H. W. *Macromolecules* **1999**, *32*, 4686–4691.

MA047885+